Ethylene Oligomerization Catalyzed by a Unique Phosphine−Oxazoline Palladium(II) Complex. Propagation and Chain Transfer Mechanisms

Mark D. Doherty, Stéphane Trudeau, Peter S. White, James P. Morken, and Maurice Brookhart*

Department of Chemistry, The University of North Carolina at Chapel Hill, Chapel Hill, North Carolina 27599

Received November 7, 2006

Palladium(II)-catalyzed ethylene oligomerization reactions using a new [(P^N)Pd(CH_3)(NCAr$_F$)][SbF_6] complex, **2b** (P^N = phosphine−oxazoline, Ar$_F$ = 3,5-(CF_3)$_2$$C_6H_3$), are described. Analysis of the X-ray crystal structure of the (P^N)Pd(CH_3)Cl precatalyst, **2a**, reveals a unique axial Pd···H interaction (2.33 Å) with a ligand C_{sp3}−H bond. Exposure of this complex to ethylene in methylene chloride produces a Schulz−Flory distribution of α-olefins ranging from C_4 to C_{24}. Effects of varying ethylene pressure and reaction temperature on oligomerizations are reported. The turnover frequency exhibits saturation behavior as ethylene pressure is increased; carrying out a Lineweaver−Burk analysis provides a barrier of 17.5 kcal/mol for migratory insertion of the palladium alkyl ethylene species. The invariance of the Schulz−Flory constant with added quantities of nitrile suggests that chain transfer occurs through a process best described as chain transfer to monomer. The catalyst resting state is shown to vary as a function of ethylene pressure and nitrile concentration. Oligomerization experiments performed with a related phosphine−oxazoline complex lacking Pd···H−C_{sp3} axial interaction lead only to ethylene dimerization.

Introduction

The polymerization of ethylene and α-olefins using late transition metal complexes has been an active area of research over the last decade.[1−5] Most thoroughly studied have been cationic Ni(II) and Pd(II) aryl-substituted α-diimine complexes bearing ortho substituents, which are effective catalysts for the polymerization of ethylene and α-olefins to high molecular weight materials through a coordination−insertion mechanism.[1−10] The orthogonal orientation of the two N-aryl rings with respect to the metal square plane positions the ortho substituents above and below the axial coordination sites of the metal. This feature has been shown to be responsible for inhibiting chain transfer relative to chain propagation, thus resulting in polymer formation from ethylene and other olefinic monomers.[3,7,11−17]

The concept of incorporating steric bulk into the axial sites of d^8 square-planar complexes to inhibit chain transfer has provided a design feature that has been used to prepare several other polymerization and oligomerization catalysts. Highly active neutral Ni(II) catalysts for ethylene polymerization have been prepared from monoanionic salicylaldiminato ligands bearing an ortho-disubstituted N-aryl ring.[18,19] Similar systems based on anilinotropone and related ligands also polymerize ethylene to give high molecular weight polymers with low molecular weight distributions.[20−23] Other related Pd(II) systems for ethylene polymerization/oligomerization that incorporate one or two ortho-disubstituted aryl groups into the ligand backbone include bis-aryl-substituted phosphindene (P^P) complexes (polymerization),[24] mixed aryl phosphinidene−arylimine (P^N) complexes (oligomerization),[25] arylimine−phosphine (N^P)

* Corresponding author. E-mail: mbrookhart@unc.edu.

(1) Britovsek, G. J. P.; Gibson, V. C.; Wass, D. F. *Angew. Chem., Int. Ed.* **1999**, *38*, 428−447.
(2) Gibson, V. C.; Spitzmesser, S. K. *Chem. Rev.* **2003**, *103*, 283−315.
(3) Ittel, S. D.; Johnson, L. K.; Brookhart, M. *Chem. Rev.* **2000**, *100*, 1169−1203.
(4) Mecking, S. *Angew. Chem., Int. Ed.* **2001**, *40*, 534−540.
(5) Mecking, S. *Coord. Chem. Rev.* **2000**, *203*, 325−351.
(6) Johnson, L. K.; Mecking, S.; Brookhart, M. *J. Am. Chem. Soc.* **1996**, *118*, 267−268.
(7) Johnson, L. K.; Killian, C. M.; Brookhart, M. *J. Am. Chem. Soc.* **1995**, *117*, 6414−6415.
(8) Leatherman, M. D.; Svejda, S. A.; Johnson, L. K.; Brookhart, M. *J. Am. Chem. Soc.* **2003**, *125*, 3068−3081.
(9) Mecking, S.; Johnson, L. K.; Wang, L.; Brookhart, M. *J. Am. Chem. Soc.* **1998**, *120*, 888−899.
(10) Svejda, S. A.; Johnson, L. K.; Brookhart, M. *J. Am. Chem. Soc.* **1999**, *121*, 10634−10635.
(11) Gates, D. P.; Svejda, S. A.; Onate, E.; Killian, C. M.; Johnson, L. K.; White, P. S.; Brookhart, M. *Macromolecules* **2000**, *33*, 2320−2334.
(12) Tempel, D. J.; Johnson, L. K.; Huff, R. L.; White, P. S.; Brookhart, M. *J. Am. Chem. Soc.* **2000**, *122*, 6686−6700.
(13) Shultz, L. H.; Tempel, D. J.; Brookhart, M. *J. Am. Chem. Soc.* **2001**, *123*, 11539−11555.
(14) Deng, L.; Margl, P.; Ziegler, T. *J. Am. Chem. Soc.* **1997**, *119*, 1094−1100.
(15) Deng, L.; Woo, T. K.; Cavallo, L.; Margl, P. M.; Ziegler, T. *J. Am. Chem. Soc.* **1997**, *119*, 6177−6186.
(16) Michalak, A.; Ziegler, T. *Organometallics* **2000**, *19*, 1850−1858.
(17) Woo, T. K.; Margl, P. M.; Blöchl, P. E.; Ziegler, T. *J. Phys. Chem. B* **1997**, *101*, 7877−7880.
(18) Younkin, T. R.; Connor, E. F.; Henderson, J. I.; Friedrich, S. K.; Grubbs, R. H.; Bansleben, D. A. *Science* **2000**, *287*, 460−462.
(19) Wang, C.; Friedrich, S.; Younkin, T. R.; Li, R. T.; Grubbs, R. H.; Bansleben, D. A.; Day, M. W. *Organometallics* **1998**, *17*, 3149−3151.
(20) Jenkins, J. C.; Brookhart, M. *Organometallics* **2003**, *22*, 250−256.
(21) Hicks, F. A.; Jenkins, J. C.; Brookhart, M. *Organometallics* **2003**, *22*, 3533−3545.
(22) Hicks, F. A.; Brookhart, M. *Organometallics* **2001**, *20*, 3217−3219.
(23) Jenkins, J. C.; Brookhart, M. *J. Am. Chem. Soc.* **2004**, *126*, 5827−5842.
(24) Ikeda, S.; Ohhata, F.; Miyoshi, M.; Tanaka, R.; Minami, T.; Ozawa, F.; Yoshifuji, M. *Angew. Chem., Int. Ed.* **2000**, *39*, 4512−4513.
(25) Daugulis, O.; Brookhart, M.; White, P. S. *Organometallics* **2002**, *21*.

10.1021/om061025v CCC: $37.00
Publication on Web 01/20/2007

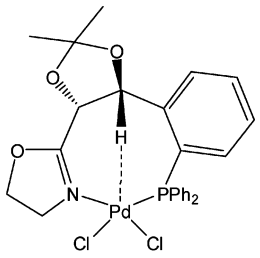

1

Figure 1. (phosphine−oxazoline)$PdCl_2$.

complexes (oligomerization),[26] arylphosphinidene−thioaryl (P^S) complexes (oligomerization/polymerization),[25] and phenacylphosphine (P^O) complexes (oligomerization).[27,28]

A number of bidentate Pd(II) complexes lacking ligand substitution patterns that place substituents near axial sites prove to be simple ethylene dimerization catalysts.[29−33] For example protonation of the (1,10-phenanthroline)$PdMe_2$ complex generates an ethylene dimerization catalyst in which the resting state is the ethyl ethylene complex (1,10-phenanthroline)Pd$(C_2H_4)(CH_2CH_3)^+$. Several simple bidentate phosphine Pd(II) complexes also exhibit dimerization catalysis.[32,33] In cases where substituents on phosphorus are small, the ethyl ethylene complex, (P^P)Pd$(C_2H_4)(CH_2CH_3)^+$, is the resting state, but in cases where phosphorus bears larger substituents the agostic ethyl complex, (P^P)Pd$(CH_2CH_2$-μ-H$)^+$, is the resting state and the turnover frequency is first-order in ethylene.[32]

In connection with other research,[34] the (phosphine−oxazoline)palladium(II) dichloride complex, **1**, shown in Figure 1, was synthesized. Examination of the X-ray crystal structure revealed an axial interaction between the C_{sp3}−H bond of the ligand backbone and the palladium with a Pd···H separation of 2.32 Å and a Pd···H−C_{sp3} angle of 144.3°. Upon coordination to palladium, the ^{1}H NMR chemical shift of the benzylic proton exhibits a large downfield shift from 6.15 to 9.42 ppm ($\Delta\delta$ = 3.27 ppm) and exhibits phosphorus coupling ($^2J_{H,P}$ = 2.6 Hz). These observations are consistent with those for Pt(II)[35−40] and Pd(II)[41,42] complexes possessing similar M···H−C interactions, which are best described as three-center, four-electron interactions.

Given that the presence of axial bulk has a significant impact on catalyst reactivity, the axial Pd···H interaction of **1** led us to wonder if this axial interaction would provide sufficient steric bulk to effectively retard chain transfer and result in oligomerization or polymerization of ethylene. We report here the synthesis of new (phosphine−oxazoline)palladium(II) complexes related to **1** and mechanistic studies of their activity as ethylene oligomerization catalysts.

Results

Synthesis of [(L^L′)Pd(CH_3)(NCAr$_F$)][A] (A = SbF_6, $B(Ar_F)_4$; Ar$_F$ = 3,5-$(CF_3)_2C_6H_3$) Complexes. Treatment of (COD)PdMeCl with the appropriate bidentate ligand (**2**−**4**) led to isolation of the corresponding (L^L′)PdMeCl complexes, **2a**−**4a**, as light yellow solids, which have been fully characterized by ^{1}H, ^{13}C, and ^{31}P{^{1}H} NMR spectroscopy as well as X-ray crystallography (Scheme 1). In complex **2a** the ^{1}H NMR chemical shift of the benzylic hydrogen is shifted downfield with respect to the free ligand at 8.83 ppm ($\Delta\delta$ = 2.68 ppm) and coupled to phosphorus ($^2J_{HP}$ = 4 Hz), analogous to complex **1**. The CH_3 signals for **2a** and **3a** appear at 0.62 ppm ($^3J_{HP}$ = 4 Hz) and 0.41 ppm ($^3J_{HP}$ = 3 Hz), respectively, as doublets due to phosphorus coupling, while the CH_3 signal for **4a** appears at 1.19 ppm as a singlet.

Single crystals of **2a** and **3a** suitable for X-ray diffraction analysis were obtained by slow evaporation of dichloromethane-d_2 and dichloromethane solutions, respectively. An ORTEP drawing and key bond distances and angles of **2a** are given in Figure 2, while those for **3a** are given in Figure 3 (crystallographic data are summarized in Table 5, see Experimental Section). Both complexes are four-coordinate with square-planar geometry, the most notable features being the *cis* orientation of the methyl and phosphine ligands in both complexes as well as the axial interaction with the C−H bond of the ligand backbone in **2a** (Pd(1)−H(11) 2.33 Å, Pd(1)−H(11)−C(11) 144.1°). As with complex **1**, this interaction is most likely a result of steric constraints imparted to the ligand backbone upon coordination to palladium.

The cationic nitrile complexes **2b** and **3b** were prepared by addition of $AgSbF_6$ and 3,5-bis(trifluoromethyl)benzonitrile to methylene chloride solutions of **2a** and **3a** at room temperature (Scheme 1). The ^{1}H NMR spectrum of **2b** shows a similar downfield shift of the benzylic proton with respect to the free ligand at 8.48 ppm ($\Delta\delta$ = 2.33 ppm) as well as coupling to phosphorus ($^2J_{HP}$ = 4 Hz). Both methyl doublets in **2b** and **3b** exhibit a slight downfield shift relative to **2a** and **3a** and appear at 0.75 ppm ($^3J_{HP}$ = 2 Hz) and 0.49 ppm ($^3J_{HP}$ = 2 Hz), respectively. Signals for the bound nitrile appear at 8.31 (H_{ortho}) and 8.28 (H_{para}) ppm for **2b** and 8.38 (H_{ortho}) and 8.29 (H_{para}) ppm for **3b**. Complex **4b** can be prepared in a similar manner by treatment of **4a** with $NaB(Ar_F)_4$ and 3,5-bis(trifluoromethyl)-benzonitrile in methylene chloride at room temperature.

Ethylene Oligomerization. The results of a series of ethylene oligomerization reactions carried out in methylene chloride using catalysts **2b**−**4b** are summarized in Table 1. Complex **2b** produces a Schulz−Flory distribution of olefins containing an even number of carbons. The Schulz−Flory constant, α, represents the probability of chain propagation and is calculated from the ratio of C_{n+2}/C_n oligomers produced as shown in eq

(26) Daugulis, O.; Brookhart, M. *Organometallics* **2002**, *21*, 5926−5934.
(27) Liu, W.; Malinoski, J. M.; Brookhart, M. *Organometallics* **2002**, *21*, 2836−2838.
(28) Malinoski, J. M.; Brookhart, M. *Organometallics* **2003**, *22*, 5324−5335.
(29) Andrieu, J.; Braunstein, P.; Naud, F.; Adams, R. D. *J. Organomet. Chem.* **2000**, *601*, 43−50.
(30) An exception to this trend was reported using cationic bis(pyrazolyl)-pyridine palladium complexes as catalysts for the polymerization of ethylene. See: Mohlala, M. S.; Guzei, I. A.; Darkwa, J.; Mapolie, S. F. *J. Mol. Catal. A* **2005**, *241*, 93−100.
(31) Rix, F. C.; Brookhart, M. *J. Am. Chem. Soc.* **1995**, *117*, 1137−1138.
(32) Ledford, J.; Shultz, C. S.; Gates, D. P.; White, P. S.; DeSimone, J. M.; Brookhart, M. *Organometallics* **2001**, *20*, 5266−5276.
(33) Shultz, C. S.; Ledford, J.; DeSimone, J. M.; Brookhart, M. *J. Am. Chem. Soc.* **2000**, *122*, 6351−6356.
(34) Trudeau, S.; Morken, J. P. *Tetrahedron* **2006**, *62*, 11470−11476.
(35) Albinati, A.; Anklin, C. G.; Pregosin, P. S. *Inorg. Chim. Acta* **1984**, *90*, L37−L38.
(36) Anklin, C. G.; Pregosin, P. S. *Magn. Reson. Chem.* **1985**, *23*, 671−675.
(37) Albinati, A.; Anklin, C. G.; Ganazzoli, F.; Ruegg, H.; Pregosin, P. S. *Inorg. Chem.* **1987**, *26*, 503−508.
(38) Albinati, A.; Arz, C.; Pregosin, P. S. *Inorg. Chem.* **1987**, *26*, 508−513.
(39) Albinati, A.; Arz, C.; Pregosin, P. S. *J. Organomet. Chem.* **1988**, *356*, 367−379.
(40) Albinati, A.; Pregosin, P. S.; Wombacher, F. *Inorg. Chem.* **1990**, *29*, 1812−1817.
(41) Mann, B. E.; Bailey, P. M.; Maitlis, P. M. *J. Am. Chem. Soc.* **1975**, *97*, 1275−1276.
(42) Roe, D. M.; Bailey, P. M.; Moseley, K.; Maitlis, P. M. *J. Chem. Soc., Chem. Commun.* **1972**, 1273−1274.

Scheme 1. Synthesis of Cationic Pd(II)−CH_3 Complexes

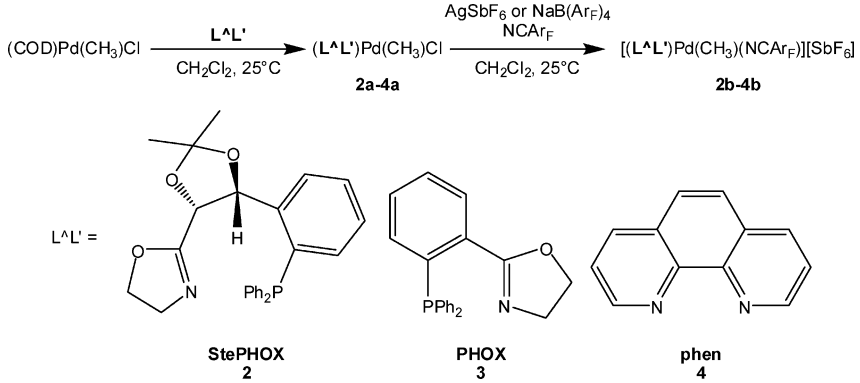

1.[43] The primary products are linear α-olefins with the remainder (up to 25%) being made up of linear 2-alkenes (as determined by GC analysis). Branched olefins are not observed under any reaction conditions examined. While complex **2b** produces a distribution of olefins, catalysis employing complexes **3b** and **4b** produces solely butenes under the reaction conditions; therefore the remainder of this section will deal with catalyst **2b**.

$$\alpha = \frac{\text{rate of propagation}}{\text{rate of propagation} + \text{rate of chain transfer}} = \frac{\text{moles of } C_{n+2}}{\text{moles of } C_n} \quad (1)$$

The oligomerization data presented in Table 1 exhibit several trends. An increase in the ethylene pressure results in higher observed turnover frequency (TOF) (entries 2, 5, and 6) while not significantly altering the α values. However, doubling the pressure (entry 2 vs 5) does not result in a doubling of the TOF, while increasing the pressure by a factor of 3.5 (entry 2 vs 6) does not result in a similar increase in the TOF. This indicates that at higher ethylene pressures the reaction is approaching saturation behavior. This approach to saturation behavior can be described using the Michaelis−Menton equation (eq 2), which can be rearranged into a linear expression (eq 3). A plot of 1/TOF versus $1/[P_{C2H4}]$, a Lineweaver−Burk plot, should yield a straight line with a *y*-intercept at $1/TOF_{MAX}$ and a slope of K_m/TOF_{MAX}. TOF_{MAX} represents the turnover frequency under conditions where the reaction is saturated in ethylene. The Lineweaver−Burk plot of data from Table 1 (entries 2, 5, and 6) as shown in Figure 4 provides a TOF_{MAX} of 3600 mol ethylene per mol Pd per hour and $k_{obs} = 1.0\ s^{-1}$ at 25 °C, which corresponds to $\Delta G^{\ddagger} = 17.5$ kcal/mol.

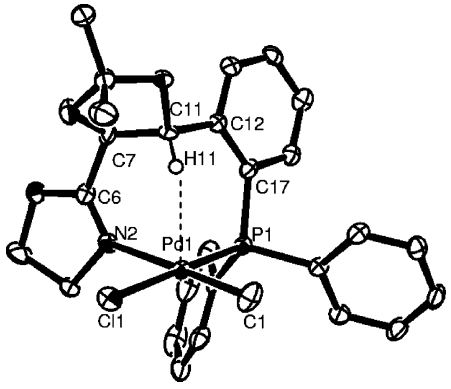

Figure 2. ORTEP structure of (StePHOX)PdMeCl, **2a**. Selected bond lengths (Å) and angles (deg): Pd(1)−C(1) 2.046(4), Pd(1)−Cl(1) 2.364(9), Pd(1)−N(2) 2.173(3), N(2)−C(6) 1.268(5), C(6)−C(7) 1.500(6), C(7)−C(11) 1.524(5), C(11)−C(12) 1.509(6), C(12)−C(17) 1.414(5), C(17)−P(1) 1.838(4), P(1)−Pd(1) 2.225-(2), Pd(1)−H(11) 2.33, H(11)−C(11) 0.98; C(1)−Pd(1)−Cl(1) 90.64(1), Cl(1)−Pd(1)−N(2) 86.90(9), N(2)−Pd(1)−P(1) 90.47-(9), P(1)−Pd(1)−C(1) 91.97(1), Pd(1)−N(2)−C(6) 132.7(3), N(2)−C(6)−C(7) 127.3(4), C(6)−C(7)−C(11) 116.6(3), C(7)−C(11)−C(12) 115.5(4), C(11)−C(12)−C(17) 123.3(4), C(12)−C(17)−P(1) 125.2(3), C(17)−P(1)−Pd(1) 117.04(1), Pd(1)−H(11)−C(11) 144.1.

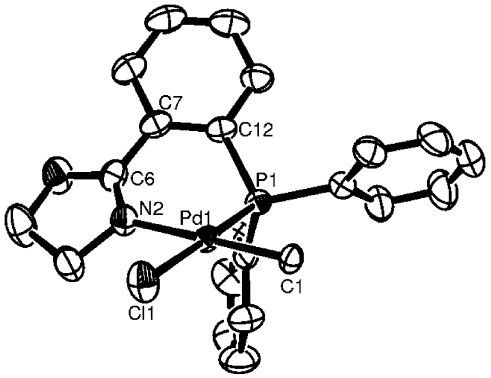

Figure 3. ORTEP structure of (PHOX)PdMeCl·CH_2Cl_2, **3a**·CH_2Cl_2. The CH_2Cl_2 has been omitted for clarity. Selected bond lengths (Å) and angles (deg): Pd(1)−C(1) 2.097(3), Pd(1)−Cl(1) 2.369-(2), Pd(1)−N(2) 2.141(3), N(2)−C(6) 1.276(4), C(6)−C(7) 1.469-(4), C(7)−C(12) 1.415(4), P(1)−C(12) 1.830(3), Pd(1)−P(1) 2.208(2); C(1)−Pd(1)−Cl(1) 88.69(1), Cl(1)−Pd(1)−N(2) 92.18-(1), N(2)−Pd(1)−P(1) 84.41(1), P(1)−Pd(1)−C(1) 94.69(1), Pd-(1)−N(2)−C(6) 130.0(2), N(2)−C(6)−C(7) 127.0(2), C(6)−C(7)−C(12) 122.4(2), C(7)−C(12)−P(1) 120.5(2), C(12)−P(1)−Pd(1) 108.48(1).

Table 1. Oligomerization of Ethylene in Methylene Chloride

entry	catalyst	[cat] ($\times 10^5$ M)	$P_{(C2H4)}$ (psig)	*T* (°C)	α[a]	time (h)	TOF[b]
1	**2b**	9.7	200	25	0.53	0.5	1310
2	**2b**	9.7	200	25	0.53	1	1560
3	**2b**	9.7	200	25	0.54	3	980
4	**2b**	9.7	200	25	0.55	8.33	790
5	**2b**	9.7	400	25	0.49	1	2260
6	**2b**	9.7	700	25	0.53	1	2560
7	**2b**	9.7	200	50	0.35	1	15 760
8	**3b**	9.7	200	25	N/A[c]	1	
9	**4b**	9.7	200	25	N/A[c]	1	

[a] Schulz−Flory α. [b]Turnover frequency = mol of ethylene consumed/mol of Pd catalyst per hour. [c]Only butenes produced.

$$V = \frac{V_{MAX}[S]}{\{K_m + [S]\}} \quad (2)$$

$$\frac{1}{V} = \frac{K_m}{V_{MAX}[S]} + \frac{1}{V_{MAX}} \quad (3)$$

An increase in reaction temperature from 25 °C to 50 °C results in a 10-fold increase in catalyst activity (entry 2 vs 7). This increase in activity is also accompanied by an increase in the rate of chain termination relative to propagation, as can be seen by the lower value of the Schulz−Flory constant, α. At longer reaction times, the catalyst activity decreases as a result of catalyst decay (Table 1, compare entries 1−4). The Schulz−Flory α values remain constant, indicating that the decomposition products, although unknown, do not significantly interfere with the oligomerization process.

Effects of Excess $NCAr_F$, Determination of K_{eq}, and $NCAr_F$ Self-Exchange Rates. Addition of excess nitrile to the reaction mixture inhibits the rate of formation of α-olefins, as can be seen by the data shown in Table 2. This decrease in activity is not accompanied by a decrease in the Schulz−Flory α value, indicating the added nitrile has not affected the ratio of chain transfer to chain propagation rates. The high concentrations of $NCAr_F$ necessary to effectively inhibit oligomerization indicate that under normal oligomerization conditions (no added nitrile) an alkyl nitrile species is present only in low concentrations relative to other species (see below).

To assess the relative binding affinities of ethylene and 3,5-bis(trifluoromethyl)benzonitrile, the equilibrium constant for the reaction shown in Scheme 2 was determined. When complex **2b** was treated with ethylene (5, 10, and 20 equiv) at −80 °C, an equilibrium mixture of **2b** and **2c** was generated and the ratio of the two complexes determined by integration of the two methyl signals at 0.600 and 0.391 ppm, respectively. Measurement at −80 °C was necessary to avoid complications from insertion chemistry of **2c** and rapid (NMR time scale) interconversion of these species due to associative ligand exchange. The measured K_{eq} was 0.13, indicating a ca. 1 order of magnitude difference in binding affinities. Since the ΔS value for this equilibrium is expected to be close to zero, the ΔG value of 0.78 kcal/mol can be used to estimate K_{eq} at higher temperatures.

The rate of exchange of bound nitrile with free nitrile was determined using line-broadening analysis of ^{1}H NMR spectra taken at low temperature (Scheme 3). The line width at half-height for the bound nitrile in **2b** in the absence of free nitrile was measured in CD_2Cl_2 at −70 °C. Line widths at half-height (ω) were measured (in Hz) in the presence of added nitrile at −70 °C. The change in line width, $\Delta\omega$, was found to be proportional to the concentration of added nitrile consistent with associative exchange. The second-order rate constants for exchange were determined using the equation for the slow exchange approximation, $k = \pi(\Delta\omega)/[NCAr_F]$, where $[NCAr_F]$ is the concentration of free nitrile in solution (Table 3). The rate data and the free energy of activation for this process are summarized in Table 3.

Synthesis and Migratory Insertion Reaction of [(StePHOX)-Pd(CH_3)(C_2H_4)][$B(Ar_F)_4$] (Ar_F = 3,5-$(CF_3)_2C_6H_3$), 2c. The precursor to complex **2c**, the palladium(II) dimethyl complex **5**, was prepared by addition of ligand **2** to a diethyl ether solution of (TMEDA)Pd(CH_3)$_2$ at −30 °C followed by warming to 25 °C overnight (TMEDA = *N*,*N*,*N*′,*N*′-tetramethylethylenediamine, Scheme 4). After workup, **5** was isolated as a light yellow solid and was characterized by ^{1}H, ^{13}C, and ^{31}P{^{1}H} NMR spectroscopy. The ^{1}H NMR spectrum of **5** shows the benzylic proton shifted downfield relative to the free ligand at 9.65 ppm ($\Delta\delta$ = 3.50 ppm) and coupled to phosphorus ($^2J_{HP}$ = 6 Hz) as in complexes **1**, **2a**, and **2b**. The two CH_3 signals appear as two doublets at 0.95 ppm ($^3J_{HP}$ = 7 Hz) and 0.88 ($^3J_{HP}$ = 9 Hz) ppm, respectively.

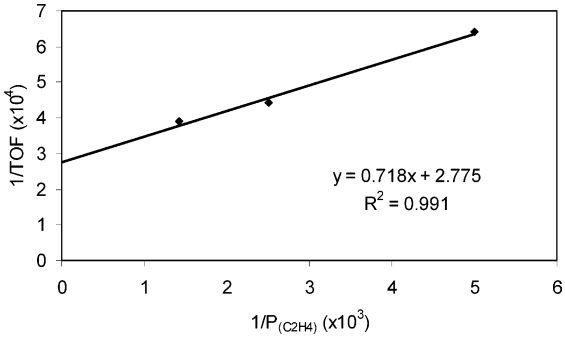

Figure 4. Lineweaver−Burk plot of ethylene oligomerization data.

Table 2. Effect of Added $NCAr_F$ on Ethylene Oligomerization

entry	$NCAr_F$ equiv[a]	$[NCAr_F]$ (×10^5 M)	α	time (h)	TOF[b]
1	0	0	0.53	1	1560
2	3	29	0.51	1	1230
3	10	97	0.50	1	1380
4	50	485	0.52	2	840
5	100	970	0.52	2	750
6	250	2425	0.53	2	610
7	500	4850	0.52	2	380

[a] Reaction conditions: **[2b]** = 9.7 × 10^{-5} M, 200 psig of ethylene, 25 °C, 100 mL of CH_2Cl_2. [b]TOF = mol of ethylene consumed/mol of Pd catalyst per hour.

Protonation of a CD_2Cl_2 solution of **5** with $[H(OEt_2)_2][B(Ar_F)_4]$ at −78 °C followed by addition of 20 equiv of ethylene generated the palladium(II) methyl ethylene complex **2c** (Scheme 4). The rate of the migratory insertion reaction of **2c** was monitored by measuring the disappearance of the palladium methyl resonance in the ^{1}H NMR spectrum at −21, −15, and −10 °C. Data are summarized in Table 4. First-order kinetics is observed with an average free energy of activation, $\Delta G^{\ddagger}$, of 19.8 kcal/mol. The subsequent rates of migratory insertions of higher homologues, (L^L)Pd($(CH_2)_nCH_3$)(C_2H_4)$^+$, must be considerably faster since ethylene is consumed at a much faster rate than the decrease of the methyl signal of **2c**. This considerable difference in rate precluded a quantitative measurement of the rate of subsequent insertion(s) by NMR spectroscopy.

Discussion

The ethylene oligomerization results presented in Table 1 illustrate the effect of the axial C_{sp3}-H···Pd interaction on the reactivity of palladium(II) complex **2b**. Complexes **3b** and **4b**, both of which lack any axial bulk, produce butenes, while complex **2b** produces linear α-olefins up to C_{24}. The proposed oligomerization mechanism for this reaction is similar to that of related late metal systems[43,44] and can be broken up into three parts: initiation, propagation, and chain transfer. The first insertion constitutes the "initiation" step and must involve migratory insertion of the methyl ethylene complex **2c**. Given

(43) Svejda, S. A.; Brookhart, M. *Organometallics* **1999**, *18*, 65−74.

(44) Killian, C. M.; Johnson, L. K.; Brookhart, M. *Organometallics* **1997**, *16*, 2005−2007.

Scheme 2. Determination of K_{eq}

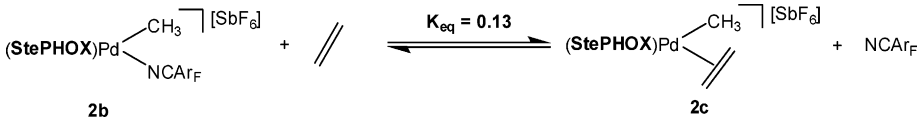

Scheme 3. Associative Exchange of 2b with Free $NCAr_F$

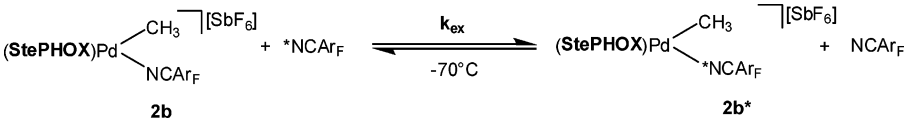

Scheme 4. Synthesis of the Cationic Pd(II) Methyl Ethylene Complex

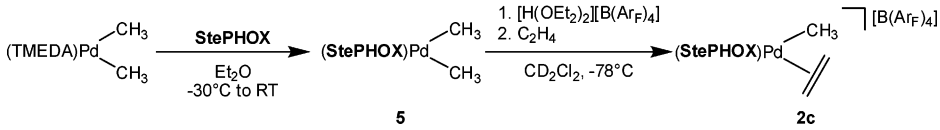

Scheme 5. Kinetics of Migratory Insertion in 2c

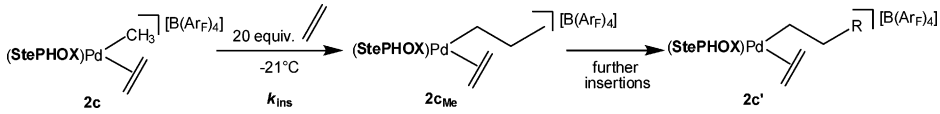

the relative binding affinities of ethylene and 3,5-bis(trifluoromethyl)benzonitrile $K_{eq} \approx 0.27$ (extrapolated from −80 °C), at 25 °C, 200 psi of ethylene, the methyl ethylene complex **2c** must be the major species in solution (**2c**/**2b** ≈ 6800).[45] Migratory insertion generates a propyl complex that can undergo chain transfer to yield propylene or further insertions and chain transfer to yield odd carbon number oligomers. Once an odd oligomer is produced, the catalyst enters the primary propagation cycle, which is described in Scheme 6. Since hundreds of turnovers are achieved prior to analysis of products, the small fraction of odd oligomers are not a significant fraction of the product and are not detected.

Scheme 6 is consistent with the dependence of the TOF on ethylene pressure and the approach to saturation as established by the Lineweaver−Burk plot. The ratio of the maximum TOF (ca. 3600 s^{-1}) to the observed TOF at 200 psi ethylene (ca. 1500 s^{-1}) suggests that ca. 40% of the palladium complex under these conditions is present as alkyl ethylene complex **2c′**. The remainder of the palladium complexes must be an equilibrium mixture of the nitrile complex **2b′** and the agostic alkyl complex **2d**. It is possible that the agostic alkyl complexes are in equilibrium with olefin hydride complex **2e′**, but experimental[12,13,46] and theoretical[14,15,47,48] studies on related complexes suggest the more stable form is the β-agostic species. The addition of free nitrile retards the rate as the equilibrium shifts from the ethylene complex to the nitrile complex. The fact that a large excess of nitrile is necessary to significantly reduce the TOF (see Table 2) implies that under conditions where only 1 equiv is present (Table 1) the nitrile complex is present in very low concentrations relative to the ethylene complex **2c′**, and thus the primary species present in addition to **2c′** is the agostic species **2d**.

The TOF_{MAX}, 1.0 s^{-1}, is the rate constant of migratory insertion of **2c′** at 25 °C and corresponds to a $\Delta G^{\ddagger} = 17.5$ kcal/mol. The $\Delta G^{\ddagger}$ for migratory insertion of the methyl ethylene complex **2c** is ca. 19.8 kcal/mol in the temperature range −10 to −21 °C. This difference is consistent with the observation (see above) that subsequent insertions occur at faster rates than the insertion of the methyl complex and with previous observations of methyl versus ethyl migratory insertion rates.[13,46]

Insight into the chain transfer mechanism can be gleaned from the data in Tables 1 and 2. Data in Table 1 indicate there is no dependence of the Schulz−Flory α value on ethylene concentration. This is consistent with a chain transfer mechanism involving either associative displacement of an olefin from an

Table 3. Second-Order Rate Constants for Nitrile Exchange at −70 °C

[**2b**] (M)	[$NCAr_F$] (M)	rate const (M^{-1} s^{-1})	$\Delta G^{\ddagger}$ (kcal/mol)
8.09×10^{-3}	7.90×10^{-3}	8.87×10^{2}	9.3
8.09×10^{-3}	3.25×10^{-2}	1.17×10^{3}	9.3

Table 4. First-Order Rate Constants for Ethylene Insertion in 2c

T (°C)	k_{ins} ($\times 10^5$ s^{-1})	$\Delta G^{\ddagger}$ (kcal/mol)
−10	16.3	19.9
−15	10.0	19.8
−21	5.3	19.6

Table 5. Crystallographic Data for 2a and 3a

	2a	**3a**·CH_2Cl_2
formula	$C_{27}H_{29}ClNO_3PPd$	$C_{23}H_{23}Cl_3NOPPd$
fw	588.33	573.14
cryst syst	orthorhombic	monoclinic
space group	$P2_12_12_1$	$P2_1/c$
a (Å)	9.6232(4)	13.245(18)
b (Å)	11.1381(5)	10.760(11)
c (Å)	24.2794(10)	17.492(12)
α (deg)	90	90
β (deg)	90	102.08(8)
γ (deg)	90	90
V (Å^3)	2602.37(19)	2438(4)
Z	4	4
D_{calcd} (Mg/m^3)	1.502	1.562
λ (Å)	0.71073	0.71073
μ (mm^{-1})	0.906	1.171
cryst dimens (mm^3)	0.20 × 0.20 × 0.10	0.30 × 0.25 × 0.10
T (K)	100(1)	298(2)
2 θ range (deg)	1.68−26.00	1.57−28.15
no. of rflns	26 615	47 387
no. of indep rflns	5111	5921
R_1	0.0378	0.0347
wR_2	0.0867	0.0821
R_{all}	0.0438	0.0399
GOF	1.063	1.139

Scheme 6. Proposed Mechanism of Ethylene Oligomerization: Propagation

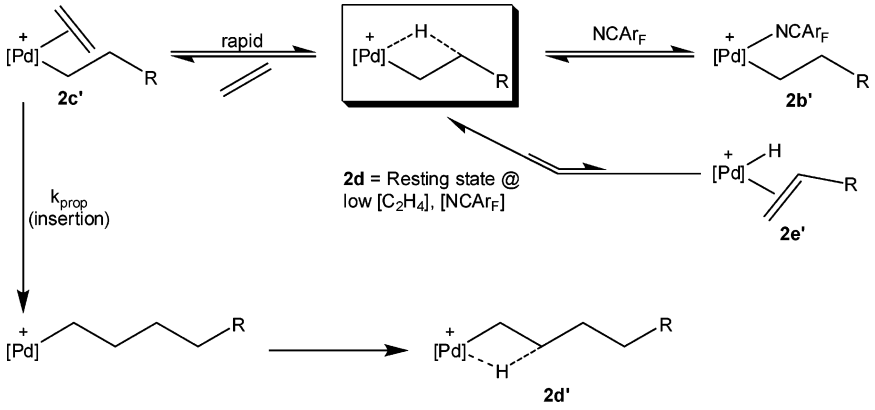

Scheme 7. Proposed Mechanism of Ethylene Oligomerization: Chain Transfer

Associative Displacement:

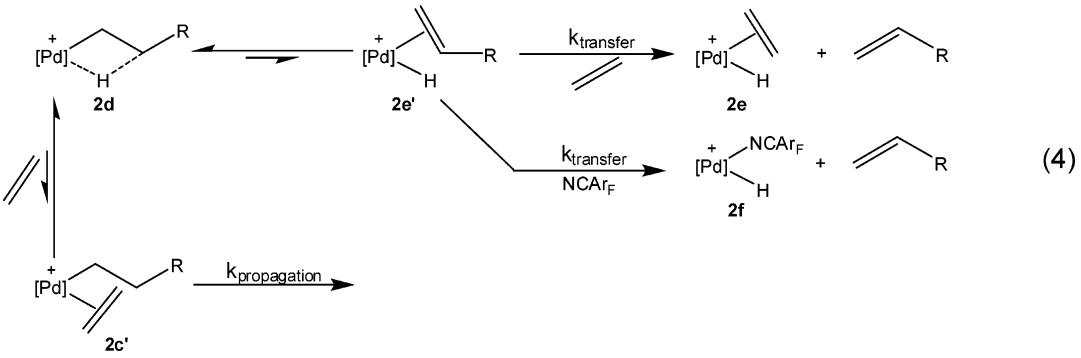

(4)

Chain Transfer to Monomer:

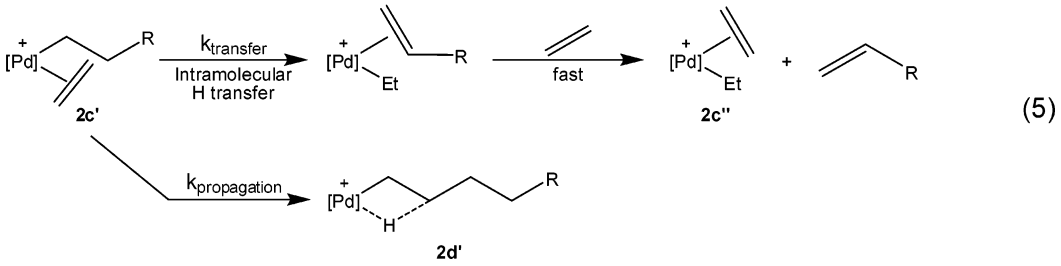

(5)

olefin hydride (eq 4) or chain transfer to monomer in which olefin displacement occurs following intramolecular hydrogen transfer in the alkyl ethylene complex (eq 5). Clearly in the chain transfer to monomer mechanism there will be no dependence of α on ethylene concentration. The ratio of transfer to propagation rates is simply the ratio of the two first-order rate constants shown in eq 5. Concerning the associative displacement mechanism, the ratio of the rates of chain transfer to propagation is given by eq 6. Since the ethylene complex **2c′** is in equilibrium with the olefin hydride complex **2e′** (eq 4, [**2e′**] = K_{eq}[**2c′**]/[C_2H_4]), eq 6 reduces to eq 7, and there is no dependence of α on ethylene concentration. Thus, in the absence of added nitrile, the data do not distinguish between the two chain transfer mechanisms.

The fact that the Schulz−Flory α value is unaffected by even extremely high concentrations of nitrile (500 equiv, Table 2) eliminates the associative displacement mechanism. Since the nitrile has an order of magnitude stronger binding affinity than ethylene and since we have established that associative self-exchange in the nitrile complex **2b** is extremely facile, olefin hydride complexes **2e′** should react rapidly with the nitrile to produce the nitrile hydride complex **2f** (eq 4). This provides another competitive "associative displacement" pathway for chain transfer (the nitrile hydride would reenter the catalytic cycle) and the α value would decrease rapidly with an increase in nitrile concentration, which is inconsistent with data in Table 2. Increase in nitrile concentration as noted above will decrease the concentration of ethylene complex **2c′** but will *not effect* the ratio of $k_{propagation}/k_{transfer}$ in eq 5 and thus will not impact α in the chain transfer to monomer mechanism, consistent with our observations.

$$\alpha = \frac{\nu_{transfer}}{\nu_{propagation}} = \frac{k_{transfer}[\mathbf{2e'}][C_2H_4]}{k_{insertion}[\mathbf{2c'}]} \qquad (6)$$

(45) An ethylene concentration of 0.18 M atm^{-1} at 25 °C in methylene chloride and the maximum possible concentration of free nitrile under oligomerization conditions of 9.7 × 10^{-5} M (see Table 1) were used together with the equilibrium constant estimated at 25 °C, K_{eq} = 0.27 (see Scheme 2), to estimate the **2c**/**2b** ratio of ca. 6800 under oligomerization conditions. The solubility of ethylene in methylene chloride at 25 °C at elevated pressures was determined previously (see ref 9).

(46) Shultz, L. H.; Brookhart, M. *Organometallics* **2001**, *20*, 3975−3982.
(47) Musaev, D. G.; Froese, R. D. J.; Svensson, M.; Morokuma, K. *J. Am. Chem. Soc.* **1997**, *119*, 367−374.
(48) Musaev, D. G.; Svensson, M.; Morokuma, K.; Strömberg, S.; Zetterberg, K.; Siegbahn, P. E. M. *Organometallics* **1997**, *16*, 1933−1945.

$$\frac{k_{\text{transfer}}K_{\text{eq}}[\mathbf{2c'}][C_2H_4]}{k_{\text{insertion}}[\mathbf{2c'}][C_2H_4]} = \frac{k_{\text{transfer}}K_{\text{eq}}}{k_{\text{insertion}}} \quad (7)$$

Conclusions

A new phosphine−oxazoline palladium(II) catalyst bearing an axial Pd···H interaction has been developed for ethylene oligomerization. The oligomers produced are linear olefins of which the majority (>75%) are α-olefins with a Schulz−Flory α value of ∼0.5 at 25 °C. The proposed mechanism of oligomerization beginning with methyl nitrile complex **2b**, [(P^N)Pd(CH_3)(NCAr_F)][SbF_6] (P^N = phosphine−oxazoline, Ar_F = 3,5-$(CF_3)_2C_6H_3$), involves insertion of ethylene into a Pd−CH_3^+ bond to generate a propyl complex (initiation), which can undergo chain transfer to yield propylene or further insertions and chain transfer to yield odd carbon number oligomers.

Following the first chain transfer event, the catalyst enters the primary propagation cycle. The major palladium complexes present under oligomerization conditions are the alkyl agostic species, **2d**, and the alkyl ethylene species, **2c′**, and their ratios depend on ethylene pressure. The turnover frequency varies with ethylene pressure and follows Michaelis−Menton kinetics. Analysis of this data using a Lineweaver−Burk plot provides a maximum TOF of 3600 h^{-1} at ethylene saturation, which corresponds to the rate of migratory insertion of the intermediate palladium alkyl ethylene complex **2c′** (k_{obs} = 1.0 s^{-1}, $\Delta G^{\ddagger}$ = 17.5 kcal/mol at 25 °C). This barrier is consistent with the insertion barrier of $\Delta G^{\ddagger}$ = 19.8 kcal/mol.

The insensitivity of the Schulz−Flory α value to variations in ethylene pressure and nitrile concentration together with the similar binding affinities of nitrile and ethylene and rapid associative nitrile exchange strongly suggest that chain transfer occurs via a "chain transfer to monomer" mechanism rather than by associative displacement of olefin from an olefin hydride complex.

Ethylene oligomerization performed with complex **3b**, which has similar electronic properties to **2b** but lacks the axial C−H···Pd interaction, yields strictly butenes. Other related Pd complexes lacking substituents that shield the axial site also show only dimerization activity. These observations highlight the significance of the axial bulk provided by the ligand C_{sp3}−H bond in **2b**.

Experimental Section

General Methods. All manipulations of air- and/or moisture-sensitive compounds were conducted using standard Schlenk techniques. Argon was purified by passage through columns of BASF R3-11 catalyst (Chemalog) and 4 Å molecular sieves. Toluene, pentane, hexane, methylene chloride, and diethyl ether were deoxygenated and dried over a column of activated alumina.

Materials. 1,5-Cyclooctadiene, 3,5-bis(trifluoromethyl)benzonitrile, 1,10-phenanthroline, and $AgSbF_6$ were used as received from Aldrich. Na[B(Ar_F)$_4$] was purchased from Boulder Scientific and purified according to reported procedures.[49] (COD)PdMeCl,[50] (TMEDA)Pd(CH_3)$_2$,[51] H(OEt_2)$_2$B(Ar_F)$_4$[52] (Ar_F = 3,5-$(CF_3)_2C_6H_3$), **2**,[34] and **3**[53−55] were prepared according to literature procedures. Polymer grade ethylene (99.9%) was purchased from Matheson and used as received. Methylene chloride-d_2, toluene-d_8, and chloroform-*d* were purchased from Cambridge Isotope Laboratories, degassed using freeze−pump−thaw techniques, and stored over 4 Å molecular sieves. GC analysis was performed on an Agilent 6850 Series GC System using a J. & W. Scientific HP-1 column (100% dimethylpolysiloxane, 30 m × 0.32 mm i.d., 0.25 μm film thickness; temperature progression: 3 min isothermal at 50 °C, 10 °C/min heat up, 3 min isothermal at 250 °C). All ^{1}H, ^{13}C, ^{19}F, and ^{31}P NMR spectra were recorded on Bruker Avance 300, 400, or 500 MHz spectrometers. Chemical shifts are reported relative to residual $CHCl_3$ (δ 7.27 for ^{1}H), $CHDCl_2$ (δ 5.32 for ^{1}H), C_6D_5-CHD_2 (quintet centered at δ 2.09, J = 2.3 Hz for ^{1}H), CD_2Cl_2 (δ 54.00 for ^{13}C), $C_6D_5CD_3$ (δ 20.4 for ^{13}C), and $CFCl_3$ (δ 0.00 ^{19}F).

(StePHOX)Pd(CH_3)Cl, 2a. A flame-dried Schlenk flask was charged with (COD)PdMeCl (0.100 g, 0.377 mmol) and methylene chloride (4 mL). A solution of ligand **2** (0.173 g, 0.399 mmol) in methylene chloride (6 mL) was added by cannula. The clear solution was stirred at room temperature for approximately 1 h. The yellow solution was then concentrated in vacuo to ∼1−2 mL, and hexane (20 mL) was added to precipitate **2a** as a light yellow solid. The solid was washed with hexane (2 × 5 mL) and dried in vacuo at room temperature for 2 h (0.194 g, 87%). X-ray quality crystals were grown via slow evaporation of methylene chloride-d_2 from a concentrated solution of **2a**. ^{1}H NMR (CD_2Cl_2, 400 MHz): δ 8.83 (1H, dd, $^3J_{HH}$ = 8 Hz, $^2J_{HP}$ = 4 Hz), 7.97 (1H, dd), 7.63 (1H, t), 7.60 to 7.20 (11H, m), 7.10 (1H, t), 4.23 (2H, overlapping m), 3.98 (1H, dd), 3.74 (1H, m), 2.79 (1H, m), 1.68 (3H, s), 1.67 (3H, s), 0.620 (3H, d, $^3J_{HP}$ = 4 Hz). ^{13}C NMR (CD_2Cl_2, 100.6 MHz): δ 165.3, 143.2, 136.9, 133.9, 133.8, 133.2, 132.6, 131.6, 131.4, 131.1, 130.9, 130.3, 129.2, 129.0, 128.7, 128.6, 128.5, 128.3, 127.8, 127.6, 112.1, 77.2, 75.7, 68.9, 26.7, 26.3, 3,68. ^{31}P{^{1}H} NMR (CD_2Cl_2, 161.9 MHz): δ 23.12 (s). Anal. Calcd for $C_{27}H_{29}PNO_3ClPd$: C, 55.12; H, 4.97; N, 2.38. Found: C, 55.47; H, 4.94; N, 2.33.

(PHOX)PdMeCl, 3a. A flame-dried Schlenk flask was charged with (COD)PdMeCl (0.076 g, 0.285 mmol) and methylene chloride (4 mL). A solution of ligand **3** (0.100 g, 0.302 mmol) in methylene chloride (6 mL) was added by cannula. The clear solution was stirred at room temperature for approximately 1 h. The yellow solution was then concentrated in vacuo to ∼1−2 mL, and hexane (20 mL) was added to precipitate **3a** as a light yellow solid. The solid was washed with hexane (2 × 5 mL) and dried in vacuo at room temperature for 2 h (0.129 g, 93%). X-ray-quality crystals were obtained via slow evaporation of methylene chloride from a concentrated solution of **3a**. ^{1}H NMR (CD_2Cl_2, 300.13 MHz): δ 8.11 (1H, ddd), 7.61 (1H, tt), 7.56 to 7.41 (11H, m), 7.15 (1H, ddd), 4.45 (4H, t), 0.406 (3H, d, $^3J_{HP}$ = 3.3 Hz). ^{31}P{^{1}H} NMR (CD_2Cl_2, 121.49 MHz): δ 34.7 (s). Anal. Calcd for $C_{22}H_{21}NOPClPd\cdot CH_2Cl_2\cdot 0.25\ C_5H_{12}\cdot 0.4\ H_2O$: C, 48.85; H, 4.34; N, 2.35. Found: C,49.37; H, 4.02; N, 2.55.

(phen)PdMeCl, 4a. This complex was prepared according to previously reported procedures.[56,57] ^{1}H NMR ($CDCl_3$, 400.13 MHz): δ 9.46 (1H, bs), 8.98 (1H, bs), 8.50 (1H, d, $^3J_{HH}$ = 5 Hz), 8.43 (1H, d, $^3J_{HH}$ = 5 Hz), 7.94 (2H, bs), 7.84 (2H, bs), 1.19 (3H, s).

[(StePHOX)PdMe(3,5-NC$_6$H$_3$(CF$_3$)$_2$)][SbF$_6$], 2b. A flame-dried Schlenk flask was charged with **2a** (0.150 g, 0.255 mmol) and 3,5-$NCC_6H_3(CF_3)_2$ (0.047 mL, 0.280 mmol) in methylene

(49) Yakelis, N. A.; Bergman, R. G. *Organometallics* **2005**, *24*, 3579−3581.
(50) Ladipo, F. T.; Anderson, G. K. *Organometallics* **1994**, *13*, 303−306.
(51) de Graaf, W.; Boersma, J.; Smeets, W. J. J.; Spek, A. L.; van Koten, G. *Organometallics* **1989**, *8*, 2907−2917.
(52) Brookhart, M.; Grant, B.; Volpe, A. F. *Organometallics* **1992**, *11*, 3920−3922.
(53) Dawson, G. J.; Frost, C. G.; Williams, J. M. J.; Coote, S. J. *Tetrahedron Lett.* **1993**, *34*, 3149−3150.
(54) Sprinz, J.; Helmchen, G. *Tetrahedron Lett.* **1993**, *34*, 1769−1772.
(55) von Matt, P.; Pfaltz, A. *Angew. Chem., Int. Ed.* **1993**, *32*, 566−568.
(56) Albano, V. G.; Castellari, C.; Cucciolito, M. E.; Panunzi, A.; Vitagliano, A. *Organometallics* **1990**, *9*, 1269−1276.
(57) De Felice, V.; Albano, V. G.; Castellari, C.; Cucciolito, M. E.; De Renzi, A. *J. Organomet. Chem.* **1991**, *403*, 269−277.

chloride (2 mL). A solution of $AgSbF_6$ (0.092 g, 0.268 mmol) in methylene chloride (3 mL) was added via cannula. The solution was diluted with methylene chloride (5 mL) and stirred at room temperature. After ~30 min, the light brown precipitate (AgCl) was removed by cannula filtration and washed with methylene chloride (2 × 5 mL). The washings were combined with the light yellow filtrate and concentrated in vacuo to ~1−2 mL, and pentane (20 mL) was added to precipitate **2b** as an off-white solid. The solid was washed with pentane (2 × 5 mL) and dried in vacuo at room temperature for 2 h (0.222 g, 85%). ^{1}H NMR (CD_2Cl_2, 300.13 MHz): δ 8.48 (1H, dd, $^3J_{HH}$ = 8 Hz, $^2J_{HP}$ = 4 Hz), 8.31 (2H, s, $NCAr_F$ *o*-H), 8.28 (1H, s, $NCAr_F$ *p*-H), 8.01 (1H, dd, J_{HH} = 4.8 and 7.5 Hz), 7.72 (1H, br t, J_{HH} = 7.5 Hz), 7.67 to 7.25 (10H, m), 7.15 (2H, overlapping dd's, J = 1.0 Hz, 1.5, 8.1, and 8.1 Hz,), 4.35 (1H, m), 4.11 (1H, d, $^3J_{HH}$ = 8.1 Hz), 3.83 (2H, overlapping m's), 2.79 (1H, m), 1.73 (3H, s), 1.68 (3H, s), 0.75 (3H, d, $^3J_{HP}$ = 2.4 Hz). ^{13}C NMR (CD_2Cl_2, 75.5 MHz): δ 167.9, 141.5, 141.3, 136.9, 133.8, 133.7, 133.3, 133.2, 133.0, 132.0, 131.2, 129.7, 129.6, 129.3, 129.1, 129.0, 128.9, 128.6, 128.5, 127.9, 127.7, 126.3, 125.6, 122.2 (q, 2 *C*F$_3$,$^1J_{CF}$ = 273.4 Hz), 118.0, 112.3, 111.9, 76.8, 69.4, 26.5, 26.4, 5.8. ^{31}P{^{1}H} NMR (CD_2Cl_2, 161.9 MHz): δ 23.03 (s). ^{19}F NMR (CD_2Cl_2, 376.5 MHz): δ −64.1 (s, $NCAr_F$), −120 to −140 (br m, SbF_6). Anal. Calcd for $C_{36}H_{33}F_{12}O_3N_2PSbPd$: C, 42.03; H, 3.23; N, 2.72. Found: C, 41.82; H, 3.03; N, 2.46.

[(PHOX)PdMe(3,5-NCC$_6$H$_3$(CF$_3$)$_2$)][SbF$_6$], 3b. A flame-dried Schlenk flask was charged with **3a** (0.100 g, 0.205 mmol) and 3,5-$NCC_6H_3(CF_3)_2$ (0.038 mL, 0.225 mmol) in methylene chloride (2 mL). A solution of $AgSbF_6$ (0.074 g, 0.215 mmol) in methylene chloride (3 mL) was added via cannula. The solution was diluted with methylene chloride (5 mL) and stirred at room temperature. After ~30 min, the light brown precipitate (AgCl) was removed by cannula filtration and washed with methylene chloride (2 × 5 mL). The washings were combined with the light yellow filtrate and concentrated in vacuo to ~1−2 mL, and pentane (20 mL) was added to precipitate **3b** as an off-white solid. The solid was washed with pentane (2 × 5 mL) and dried in vacuo at room temperature for 2 h (0.153 g, 81%). ^{1}H NMR (CD_2Cl_2, 300.13 MHz): δ 8.38 (2H, s, $NCAr_F$ *o*-H), 8.29 (1H, s, $NCAr_F$ *p*-H), 8.22 (1H, ddd, J = 1.5 Hz, 4.2 Hz, 8.1 Hz), 7.72 (1H, tt, J = 1.5 Hz, 7.8 Hz), 7.65 to 7.39 (11H, m), 7.19 (1H, ddd, J = 1.5 Hz, 7.8 Hz, 11.1 Hz), 4.62 (2H, t, $^3J_{HH}$ = 9.7 Hz), 4.30 (2H, t, $^3J_{HH}$ = 9.7 Hz), 0.49 (3H, d, $^3J_{HP}$ = 2.1 Hz). ^{13}C{^{1}H} NMR (CD_2Cl_2, 125.76 MHz): δ 164.8 (1C, d, J_{CP} = 5.2 Hz), 135.3 (1C, d, J_{CP} = 2.5 Hz), 134.4 (4C, d, J_{CP} = 12.3 Hz), 133.9 (2C, br m), 133.7 (2C, q, $^2J_{CF}$ = 35.2 Hz), 133.4 (1C, d, J_{CP} = 7.5 Hz), 132.7 (1C, d, J_{CP} = 5.7 Hz), 132.6 (1C, d, J_{CP} = 21 Hz), 129.7 (6C, d, J_{CP} = 11.8 Hz), 129.2 (1C, d, J_{CP} = 11.8 Hz), 129.0 (1C, br m), 128.0 (1C, d, J_{CP} = 47.6 Hz), 127.5 (1C, d, J_{CP} = 58.5 Hz), 122.4 (2C, q, $^1J_{CF}$ = 273.4 Hz), 118.0 (1C, s), 112.3 (1C, s), 69.23 (1C, s), 56.7 (1C, s), 2.29 (1C, s). ^{31}P{^{1}H} NMR (CD_2Cl_2, 121.49 MHz): δ 36.69 (s). ^{19}F NMR (CD_2Cl_2, 376.5 MHz): δ −64.2 (s, $NCAr_F$), −120 to −140 (br m, SbF_6). Anal. Calcd for $C_{31}H_{24}F_{12}N_2OPSbPd$: C, 40.14; H, 2.61; N, 3.02. Found: C, 38.83; H, 2.43; N, 2.85.

[(phen)PdMe(3,5-NCC$_6$H$_3$(CF$_3$)$_2$)][B(Ar$_F$)$_4$], 4b. A flame-dried Schlenk flask was charged with **4a** (0.500 g, 1.48 mmol) and 3,5-$NCC_6H_3(CF_3)_2$ (0.300 mL, 1.78 mmol) in diethyl ether (20 mL). A solution of $Na[B(Ar_F)_4]$ (1.45 g, 1.63 mmol) in diethyl ether (20 mL) was added via cannula and stirred at room temperature. After ~30 min, the volatiles were removed in vacuo and the remaining residue was taken up in methylene chloride (10 mL), resulting in a light yellow solution and a light brown precipitate (NaCl). The product was isolated via cannula filtration, and the precipitate was washed with methylene chloride (2 × 5 mL). The washings were combined with the light yellow filtrate and concentrated in vacuo to ~4−5 mL, and pentane (50 mL) was added to precipitate **4b** as a light yellow oil. The mixture was stirred overnight, resulting in formation of a light yellow precipitate, which was isolated by cannula filtration, washed with pentane (2 × 5 mL), and dried in vacuo at room temperature for 2 h (2.02 g, 97%). ^{1}H NMR (CD_2Cl_2, 400.13 MHz): δ 8.94 (1H, dd, $^3J_{HH}$ = 5 Hz, $^4J_{HH}$ = 1 Hz), 8.87 (1H, dd, $^3J_{HH}$ = 5 Hz, $^4J_{HH}$ = 1 Hz), 8.67 (1H, dd, $^3J_{HH}$ = 8 Hz, $^4J_{HH}$ = 1 Hz), 8.62 (1H, dd, $^3J_{HH}$ = 8 Hz, $^4J_{HH}$ = 1 Hz), 8.44 (2H, bs), 8.39 (1H, bs), 8.08 (1H, d, 8 Hz), 8.05 (1H, d, 8 Hz), 7.96 (1H, dd, $^3J_{HH}$ = 8 Hz, $^3J_{HH}$ = 5 Hz), 7.93 (1H, dd, $^3J_{HH}$ = 8 Hz, $^3J_{HH}$ = 5 Hz), 7.72 (8H, s), 7.53 (4H, s), 1.43 (3H, s). Anal. Calcd for $C_{54}H_{26}F_{30}N_3BPd$: C, 46.19; H, 1.87; N, 2.99. Found: C, 46.08; H, 1.92; N, 2.73.

(StePHOX)PdMe$_2$, 5. A flame-dried Schlenk flask was charged with (TMEDA)$PdMe_2$ (0.075 g, 0.297 mmol) and diethyl ether (2 mL) and cooled to −30 °C. A solution of ligand **2** (0.128 g, 0.297 mmol) in diethyl ether (3 mL) was added via cannula. The solution was diluted with diethyl ether (10 mL) and stirred at −30 °C for 3 h and allowed to warm to room temperature overnight while stirring. Volatiles were removed in vacuo to give the product **5** as a yellow solid. The solid was washed with pentane (6 × 10 mL) to remove remaining starting material and dried in vacuo for 3 h (0.074 g, 44%). ^{1}H NMR (C_7D_8, 500.13 MHz): δ 9.65 (1H, dd, $^3J_{HH}$ = 7.0 Hz, $^2J_{HP}$ = 6 Hz), 8.02 (1H, dd), 7.35 to 6.75 (17H, m), 4.12 (1H, d), 3.46, (1H, q), 3.21 (1H, q), 2.87 (1H, q), 2.39 (1H, q), 1.90 (3H, s), 1.62 (3H, s), 0.95 (3H, d, $^3J_{HP}$ = 6.8 Hz), 0.88 (3H, d, $^3J_{HP}$ = 8.6 Hz). ^{13}C NMR (C_7D_8, 125.7 MHz): δ 164.4, 143.9, 137.6, 137.5, 137.2, 135.2, 135.0, 133.5, 133.4, 133.2, 132.8, 131.6, 131.2, 111.4, 77.3, 76.2, 67.3, 58.3, 54.7, 46.0, 34.5, 26.8, 26.1, 22.9, 14.4, 3.7, 2.9, −3.4. ^{31}P{^{1}H} NMR (C_7D_8, 202.45 MHz): δ 11.78 (s). Anal. Calcd for $C_{28}H_{33}O_3NPPd$: C, 59.11; H, 5.85; N, 2.46. Found: C, 58.94; H, 5.61; N, 2.50.

General Procedure for Ethylene Oligomerizations. A 300 mL Parr autoclave was heated under vacuum up to 120 °C and then was cooled to the desired reaction temperature and backfilled with argon. In the glovebox, a flame-dried Schlenk flask was charged with the catalyst, **2b** (0.010 g, 0.0097 mmol). The catalyst was dissolved in methylene chloride (15 mL), undecane was added as an internal standard (0.011 mL, 0.050 mmol), and the mixture was cannula transferred into the argon-pressurized autoclave. Fresh methylene chloride (15 mL) was added to the flask and cannula transferred into the autoclave. The reaction mixture was diluted with additional methylene chloride (70 mL), the autoclave was sealed and pressurized with ethylene to the desired level, and the stirring motor was engaged. After the predetermined reaction time, the stirring motor was stopped and the reactor was cooled to 0 °C to retain as much of the low molecular weight oligomers as possible and then vented. An aliquot was removed for GC analysis, and the reaction mixture was quenched by pouring into 200 mL of stirring methanol. Volatiles were removed on the Rotovap, and the remaining residue was analyzed by ^{1}H NMR. This procedure was used for variations in temperature, ethylene pressure, and time. For the reactions with excess 3,5-bis(trifluoromethyl)benzonitrile, the desired amount of nitrile was added to the flask prior to cannula transfer into the autoclave.

General Procedure for Nitrile Self-Exchange. An NMR tube was charged with complex **2b** (5 mg, 0.0049 mmol) and CD_2Cl_2 (600 μL) under argon and sealed with a septum. An ^{1}H NMR spectrum was recorded at RT. The tube was cooled to −80 °C, and the desired amount of 3,5-bis(trifluoromethyl)benzonitrile was added via syringe. The reaction was followed by VT-NMR over a range of 190−238 K. The line width at half-height of the signal assigned to the ortho-H of bound nitrile in **2b** (δ 8.280) was monitored as a function of temperature, and the rate of nitrile exchange was determined using the slow exchange approximation.

General Procedure for Ethylene Insertion Reactions. A screw cap NMR tube was charged with **5** (5 mg, 0.0088 mmol) and cooled to −78 °C. A solution of $[H(OEt_2)_2][B(Ar_F)_4]$ (8.9 mg, 0.0088mmol) in CD_2Cl_2 (512 μL) was cannula transferred to the NMR tube. 1,3,5-Trimethoxybenzene (88 μL, 0.1 M in CD_2Cl_2) was added to the

NMR tube via syringe as an internal standard. The tube was warmed briefly to obtain a homogeneous solution and was then placed back into the −78 °C bath. The tube was placed in the NMR probe at −80 °C, and an ^{1}H NMR spectrum was recorded of the [(StePHOX)-PdMe(OEt_2)][B(Ar_F)$_4$] complex. The tube was then removed from the probe and placed back into the −78 °C bath, and ethylene was added via syringe (4.26 mL, 0.176 mmol (20 equiv)). The sample was then warmed to the desired temperature inside the NMR probe, and insertion was monitored by ^{1}H NMR. Disappearance of the [(StePHOX)PdMe(C_2H_4)][B(Ar_F)$_4$] complex was monitored by integration of the signal corresponding to the Pd−CH_3 (δ 0.481) versus the integration of 1,3,5-trimethoxybenzene as an internal standard. A rate of insertion was calculated by plotting the natural log of the concentration of starting material versus time.

Acknowledgment. We thank the National Science Foundation (grant CHE-0615704) and NIGMS (GM 64451) for support of this work.

Supporting Information Available: A sample plot of the kinetic analysis of ethylene insertion in **2c** and CIF files giving complete crystallographic data for complexes **2a** and **3a**. This material is available free of charge via the Internet at http://pubs.acs.org.

OM061025V